The influence of α-Al$_2$O$_3$ addition on microstructure, mechanical and formaldehyde adsorption properties of fly ash-based geopolymer products

Yi Huang, Minfang Han[*]

School of Chemical & Environmental Engineering, China University of Mining and Technology, Beijing 100083, PR China

ARTICLE INFO

ABSTRACT

Fly ash-based geopolymer with α-Al$_2$O$_3$ addition were synthesized and used to remove formaldehyde from indoor air. The microstructure, mechanical and formaldehyde adsorption properties of the geopolymer products obtained were investigated. The results showed that α-Al$_2$O$_3$ addition with appropriate amount (such as 5 wt%) increased the geopolymerization extent, resulting in the increase of surface area and compressive strength. In addition, the improvement of structural ordering level for geopolymer sample with 5 wt% α-Al$_2$O$_3$ addition was found through FTIR analysis. By contrast, excessive addition (such as 10 wt%) had the opposite effect. The test of formaldehyde adsorption capacity confirmed that fly ash-based geopolymer product exhibited much better property of adsorbing indoor formaldehyde physically and chemically than fly ash itself. The surface area was an important but not unique factor influencing the adsorption capacity of geopolymers.

© 2011 Elsevier B.V. All rights reserved.

1. Introduction

Geopolymer is a new class of inorganic polymer synthesized by activation of an aluminosilicate source with an alkaline hydroxide or silicate solution at ambient temperature, which was first developed by Davidovits in the late 1970s [1]. In recent years, geopolymer materials have attracted much more attention by reason of their excellent mechanical properties, good chemical resistance, low shrinkage, environmentally friendly nature and long-term durability [2,3]. Fly ash, considered to be a waste substance is an important aluminosilicate source material for geopolymer with containing sufficient amounts of reactive alumina and silica. Fly ash-based geopolymer has been emerged as a promising new cement alternative in the field of building and construction materials [4,5].

Geopolymers consist of a polymeric Si–O–Al framework, similar to zeolites. The main difference to zeolite is geoloymers are amorphous instead of crystalline. The microstructure of geopolymers on a nanometer scale observed by TEM comprises small alumiosilicate clusters with pores dispersed within a highly porous network. The clusters sizes are between 5 and 10 nm [2]. With these specific structural characteristics, geopolymer can be used as an adsorbent with well-developed pore structure. In recent years, some researches on the removal of pollutants in water with geopolymeric adsorbents have been reported [6–8], while there are few litera-

tures, which are concerned about purifying air pollutants with this new type of adsorbent. This paper has investigated the formaldehyde (a primary indoor air pollutant in China) adsorption properties of geopolymer products as adsorbents.

It has been proved in Refs. [9,10] that lower Si/Al ratio results in larger surface area of geopolymer and is beneficial for adsorption capacity. The present study intends to use Al$_2$O$_3$ as supplementary Al source to synthesize fly ash-based geopolymer with lower Si/Al ratio. Al$_2$O$_3$ mainly has two crystalline modifications: α-Al$_2$O$_3$ and γ-Al$_2$O$_3$. α-Al$_2$O$_3$ is highly crystalline and the most thermodynamically stable form of alumina, and therefore only slowly soluble in highly concentrated alkaline solution. While γ-Al$_2$O$_3$ is much less crystalline and is easily soluble in strong alkaline solution [11]. It is well understood that aluminum component of fly ash tends to dissolve more easily than the silicon component at early stage of geopolymerization [12] so that the addition of γ-Al$_2$O$_3$ leads to very high Al concentration at this stage. However, the addition of α-Al$_2$O$_3$ can be expected to averagely adjust the Si/Al ratio at the whole stage. Therefore, the purpose of this paper is to study the influence of α-Al$_2$O$_3$ addition on the microstructure, mechanical and adsorption properties for the formaldehyde of the fly ash-based geopolymer.

2. Experimental

2.1. Materials

A raw fly ash (FA) sample was obtained from Gaojing Power Station in Beijing, China. Table 1 gives the chemical composition

* Corresponding author.
E-mail address: hanminfang@sina.com (M. Han).

Table 1
Composition of fly ash as determined by XRF analysis (mass (%)).

Element as oxide	Fly ash
SiO_2	53.7
Al_2O_3	33.2
Fe_2O_3	3.6
CaO	3.0
TiO_2	1.6
K_2O	0.8
SO_3	0.6
MgO	0.5
P_2O_5	0.4
LOI	2.6

data determined by X-ray fluorescence (XRF) of fly ash. The α-Al_2O_3 powders were supplied from Xiongdi materials Co., Ltd. in Jiyuan, China. Sodium hydroxide pellet (AR grade) was dissolved in deionised water to obtain NaOH solution. Commercial sodium silicate solution (SF) with the mole ratio of SiO_2/Na_2O of 3.2 and density of 1.38 g/cm³ was supplied by Beijing Hongxing Guangsha Chemical & Building Materials Co., Ltd., China. NaOH solution and sodium silicate solution were mixed to prepare liquid activator 24 h prior to use. Formaldehyde solution (AR, 37%), was purchased from Beijing Chemical Reagents Company, China.

2.2. Specimen preparation

The solid materials (S) were mixed with activator solutions at a const water/solid ratio of 0.3 by a blender. The pastes were rapidly casted into a cubic steel mould. Each sample was vibrated for 5 min on the vibration table and cured at 80 °C. In order to prevent the evaporation of water, the specimens were covered with plastic films during the curing process. The mould was removed after 24 h. The demoulded specimens were cured at ambient temperature for 7 days. The detailed composition data of all the samples synthesized in this study are shown in Table 2.

2.3. Characterization of geoplymer products

Compressive test was performed on MYL-300 Compressive Resistant tester (Wuxi Jianyi, China). Six samples of each formulation were tasted and the average data were reported.

Fly ash and geopolymer products were tested by X'Pert PRO MPD X-ray spectrometer (XRD, PANalytical company, Netherlands). The XRD patterns were measured from 10° to 90° 2θ at a scan rate 2°/min.

Microstructural images were obtained using a LEICAS440i ScanningElectron Microscope (SEM, Cambridge, UK) coupled with energy dispersive X-ray spectroscopy (EDXS, Oxford instruments, UK).

Fourier-transform infrared spectra were measured on an EQUINOX55 spectrometer (FTIR, Bruker company, Germany). Spectra were collected in the mid-infrared region (4000–400 cm⁻¹) after 256 scans at 2 cm⁻¹ resolution. Samples were prepared by the standard KBr (Merck) pellets method.

Table 2
Composition of geopolymer used in this study.

Sample	Solid components (by mass)	Concentration of NaOH solutions (M)	SF/S (by mass)
F1	95%FA + 5%Al_2O_3	6	0.22
F2	95%FA + 5%Al_2O_3	9	0.22
F3	95%FA + 5%Al_2O_3	12	0.22
F4	95%FA + 5%Al_2O_3	15	0.22
F5	90%FA + 10%Al_2O_3	15	0.22
F6	100%FA	15	0.22
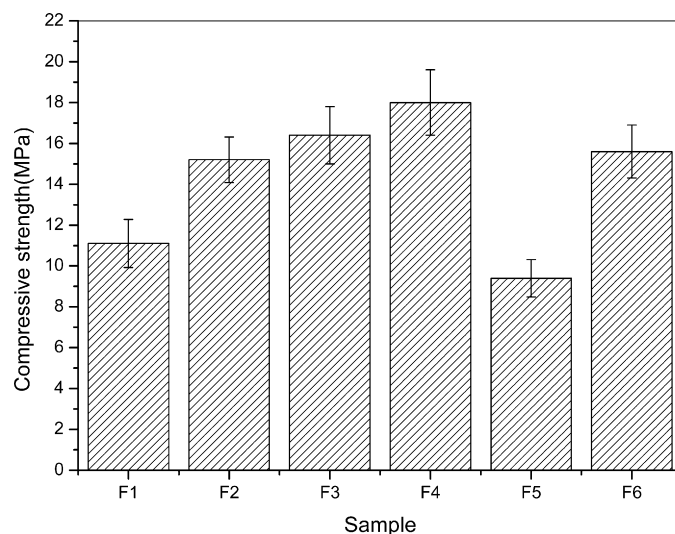
Fig. 1. Compressive strength of geopolymer products.

TG of original and formaldehyde-adsorbed geopolymer samples were performed on STA 499c DSC-TG (NETZSCH company, Germany) at a heating rate of 10 min in air from 0 to 800 °C. Formaldehyde-adsorbed geopolymer sample was obtained by setting 5 g original geopolymer sample in a 9 L desiccator full of saturated formaldehyde vapor for 24 h.

The surface area was measured by the N_2 gas adsorption BET method (Adsorb-IQ, Quantachrome, USA).

2.4. Test of formaldehyde adsorption

The geopolymer capacity for adsorbing formaldehyde was tested by static adsorption method and the sample was washed and dried before the test. The test was carried out in two 120 L glass boxes equipped with a stirrer at room temperature (25 ± 1 °C). An amount of formaldehyde solution was placed in each box to produce formaldehyde vapor and the initial concentration of formaldehyde was approximately 1.2 mg/m³. Then 250 g geopolymer sample was set in one of the two boxes and the other as control experimental box was without setting in. The stirrers were open for 1 min to mix the vapor thoroughly after the boxes were sealed. In 24 h, the concentrations of formaldehyde in the boxes were measured with PPMhtv fomaldemeter (PPM company, UK). The formaldehyde removal ratio (R) of geopolymer sample was defined as

$$R = \frac{C_2 - C_1}{C_2} \times 100\% \tag{1}$$

where C_1 and C_2 stand for the formaldehyde concentration of the box with and without geopolymer sample containing in 24 h respectively.

The Formaldehyde adsorption capacity of fly ash with the same weight was evaluated by the same method.

3. Results and discussion

3.1. Compressive strength analysis

The results of compressive strength of geopolymer products are shown in Fig. 1. For the samples with 5 wt% α-Al_2O_3 addition (F1–F4), the compressive strength increases with the increase of NaOH concentration because higher NaOH content can dissolve more raw materials and increase the amount of geopolymer gel formed [13]. With regard to samples synthesized with the same
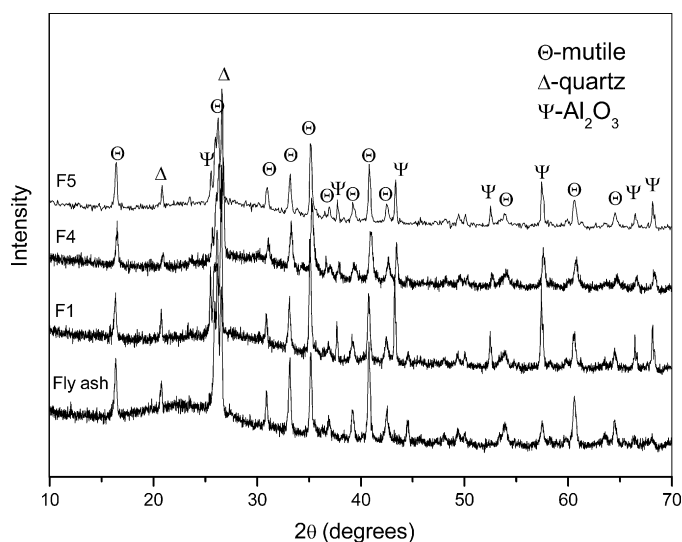
Fig. 2. XRD patterns of geopolymer products.

NaOH concentration, a moderate reduction of compressive strength for sample F6 (no α-Al$_2$O$_3$ addition) and a sharp reduction for sample F5 (10 wt% α-Al$_2$O$_3$ addition) can be found compared to sample F4 (5 wt% α-Al$_2$O$_3$ addition). It is commonly believed that compressive strength of geopolymer increases with increasing Si/Al ratio under the same synthesis conditions [10,14] and α-Al$_2$O$_3$ addition is unlikely to increase this ratio. Therefore, it can be inferred that the compressive strength improvement of sample F4 is strongly associated with the increase of geopolymerization extent.

3.2. XRD analysis

The XRD patterns of fly ash and geopolymer products are presented in Fig. 2. Quartz and mutile are the major crystalline phases in all samples that are nearly inert at the geopolymerization conditions. The main difference between XRD patterns of fly ash and geopolymer is the shift of amorphous silica peak from around 23° for original fly ash to almost 30° for geopolymer [2]. As to Al$_2$O$_3$ detectable in geopolymer samples, its peak intensity in sample F4 (5 wt% α-Al$_2$O$_3$, 15 M NaOH) is lower than that in sample F1 (5 wt% α-Al$_2$O$_3$, 6 M NaOH) and F5 (10 wt% α-Al$_2$O$_3$, 15 M NaOH). This suggests that α-Al$_2$O$_3$ can partially dissolve in alkaline activator solution as mentioned in introduction and the solubility increases with the increase of alkalinity.

3.3. SEM-EDS analysis

Fig. 3a–c gives the SEM micrographs of sample F4 (5 wt% α-Al$_2$O$_3$ addition), F5 (10 wt% α-Al$_2$O$_3$ addition) and F6 (no α-Al$_2$O$_3$ addition) respectively. There are unreacted or partially reacted fly ash particles trapped within the geopolymer phase in all samples. The results of geopolymer Si/Al ratio (Fig. 3, points 1–6) through EDS spot analysis are summarized in Table 3. The geopolymer phase

Table 3
Results of EDS spot analysis of geopolymer products.

Sample	Point	Si/Al molar ratio
F4	1	1.81
F4	2	1.41
F5	3	1.63
F5	4	1.70
F6	5	2.57
F6	6	2.52

of sample F4 has a higher Al content than sample F6 (Si/Al:1.4–1.6 for sample F4 and approximately 2.5 for sample F6 as deduced from Table 3), which indicates that aluminum component comes from α-Al$_2$O$_3$ has taken part in the geopolymeric reaction. Moreover, more compact microstructure and fewer unreacted fly ash particles can be observed for sample F4 by contrast with sample F6. This suggests appropriate α-Al$_2$O$_3$ addition favors the improvement of geopolymerization extent that provides a reason for the higher compressive strength of sample F4, as supposed in compressive strength analysis presented earlier. In addition, the geopolymer gel of sample F5 with more α-Al$_2$O$_3$ content has similar Si/Al ratio (Si/Al:1.6–1.7 for sample F5 as deduced from Table 3) to sample F4, but it appears much less homogeneous microstructure reflected in the dramatic reduction of compressive strength (Fig. 1). This may be due to the formation of octahedral Al at very high Al content [15] that cannot be incorporated into the gel network.

3.4. FTIR analysis

Fig. 4 shows the FTIR spectra of sample F4 (5 wt% α-Al$_2$O$_3$ addition), F5 (10 wt% α-Al$_2$O$_3$ addition) and F6 (no α-Al$_2$O$_3$ addition). Significant broad bands are observed at approximately 3450 cm^{-1} and 1650–1600 cm^{-1} for O–H stretching and O–H bending [9]. The peak near 450 cm^{-1} is ascribed to O–Si–O bending mode [16]. The main spectral band appears at about 1000 cm^{-1} is attributed to Si–O–T (T:Si or Al) asymmetric stretching vibration, which provides an indication of the geoplymerization degree [13]. The intensity of this band in sample F4 is observed to be the highest among all three samples. This means sample F4 contains the largest amount of geopolymer phase, which correlates well with the results of SEM analysis mentioned above. It also can be seen that this band in sample F4 and F5 exhibits sharper compared to sample F6, suggesting that the geopolymer gel of sample F4 and F5 with decreased Si/Al ratio have a better level of structural ordering [17,18]. The decrease in the wavenumber of the main Si–O–T stretching band is commonly found with the decrease of geopolymer Si/Al ratio [18,19]. This is in agreement with the observation in Fig. 4 that this band for the geopolymer of sample F4 consists of more Al component (Table 3) shifts to lower wavenumbers by 7 cm^{-1} compared to sample F6. However, the opposite trend (a shift to higher wavenumbers by 15 cm^{-1} of this band in comparison with sample F6) can be observed for the geopolymer of sample F5 with similar Si/Al ratio to sample F4 (Table 3). This contradictory finding cannot be clearly explained here and should be discussed in detail in further studies, which will be helpful for a better understanding the influence of excessive α-Al$_2$O$_3$ addition on the microstructure of geopolymers. In addition, significant differences for the three samples are observed in the region from 600 to 800 cm^{-1}. These differences indicate that these samples contain different zeolites nanocrystalline or present different cage-like structures in geopolymer framework [12]. Based on the above analysis, it can be summarized that appropriate amount of α-Al$_2$O$_3$ addition (such as 5 wt%) can reduce the Si/Al ratio in activator solution so promotes the geopolymerization and allows a greater level of structure reorganization of geopolymer gel, which can be explained by the higher ability of the gel components in high-alumina system [10]. This behavior takes positive influence on the microstructure and mechanical properties of geopolymer products.

3.5. Adsorption capacity of formaldehyde and surface area

Table 4 gives the results of formaldehyde adsorption capacity and surface area of geopolymer products and fly ash. The formaldehyde removal ratio and surface area show the similar trend as compressive strength (Fig. 1). This implies geopolymers are porous and take the main role in adsorption action so that a lager amount of
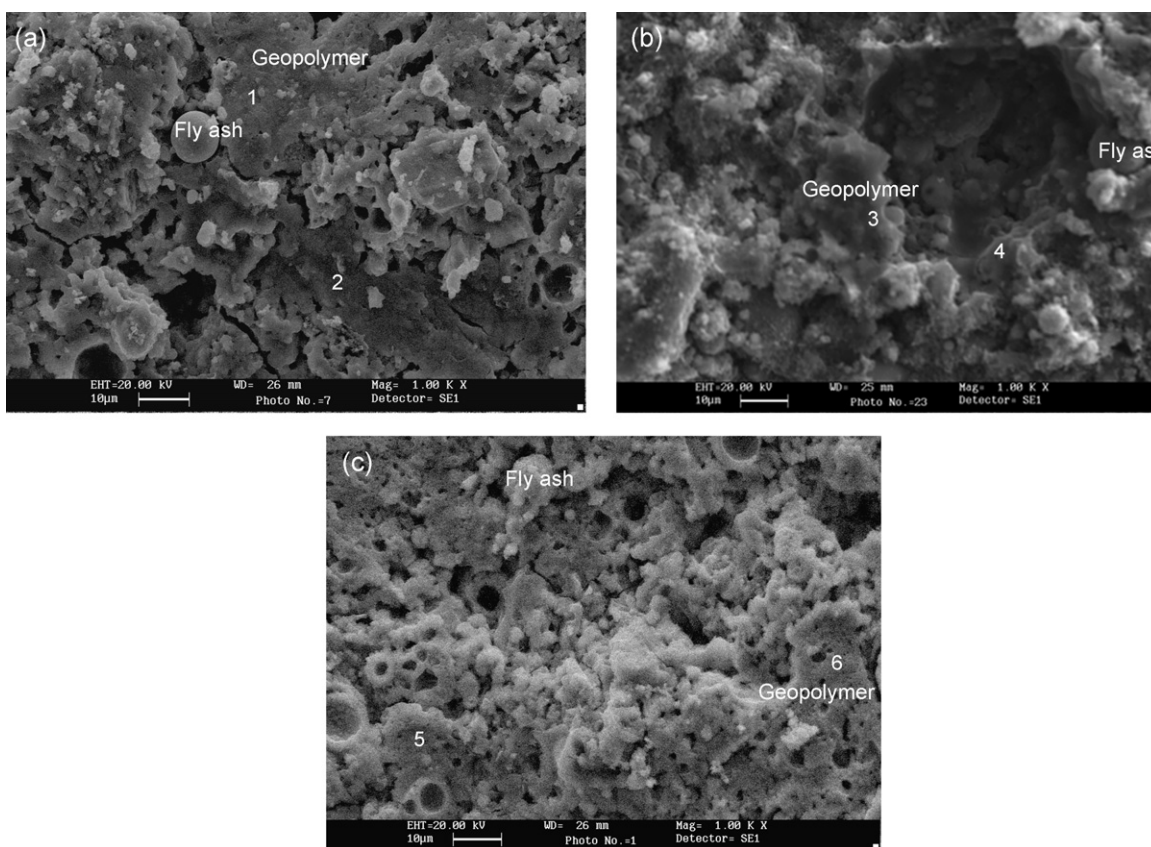
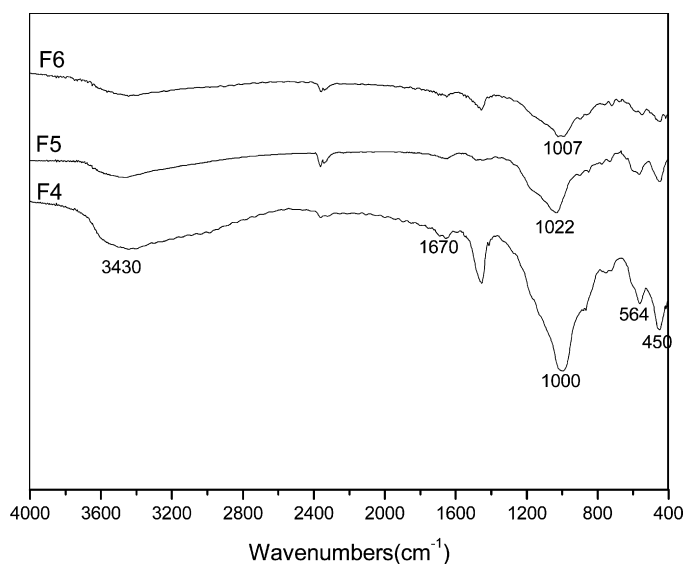**Fig. 3.** SEM images of (a) sample F4 (b), sample F5 and (c) sample F6.

Fig. 4. FTIR spectra of geopolymer products.

Table 4
Surface area and formaldehyde removal ratio of geopolymer products.

Sample	Surface area (m^2/g)	C_1 (mg/m^3)	C_2 (mg/m^3)	R (%)
Fly ash	16.62	1.15	1.02	11.3
F1	14.41	1.18	0.52	56.0
F2	22.50	1.17	0.40	65.8
F3	28.95	1.12	0.33	70.5
F4	34.26	1.10	0.24	78.2
F5	15.34	1.18	0.46	61.0
F6	21.37	1.18	0.34	71.2

geopolymer formed results in lager surface area and formaldehyde adsorption capacity. Fly ash exhibits the smallest formaldehyde removal ratio (R only 11.3%), but it is noted fly ash has larger surface area than sample F1. This suggests adsorption capacity is not only related with the surface area and chemical adsorption should be expected to take place between geopolymers and formaldehyde molecules.

Fig. 5 shows the results of thermogravimetric analysis carried out on the sample F4 before and after adsorbing formaldehyde. The thermogravimetric data of sample F4 before adsorbing in Fig. 4 show that about 55% of all water is evaporated up to
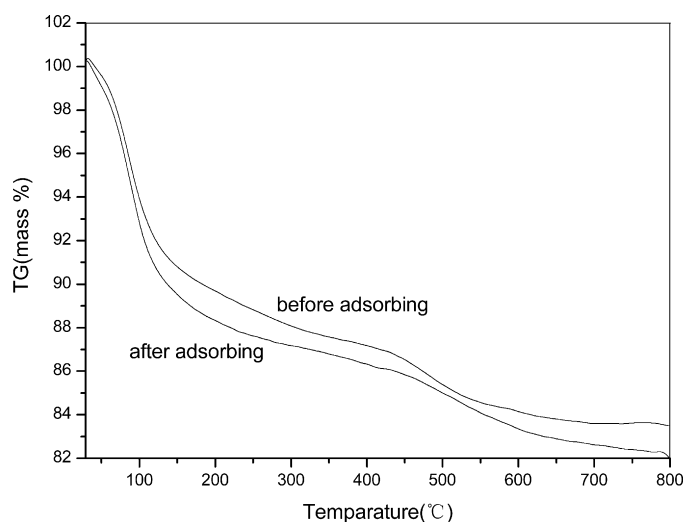

Fig. 5. TG curves of geopolymer products before and after adsorbing formaldehyde.

150 °C. The most probable water stage is the 'free' and weakly adsorbed, residing in the pores roughly above 5 nm [20]. Additional water mass is evaporated at thermal interval between 150 and 600 °C. This water comes from nano-pores of the geopolymer gel or condensation of hydroxyl groups (>300 °C) [18]. After adsorbing formaldehyde, sample F4 presents larger mass loss which is caused by the evaporation of formaldehyde mainly occurred after 120 °C. Therefore, we can believe that most of the adsorbed formaldehyde is strongly fixed on the internal surface of pores. What is more, evident differences between the two thermogravimetric curves above 250 °C can be found from Fig. 5. This may be due to the forming of hydrogen bond between formaldehyde and hydroxyl groups of geopolymers which impacts on the dehydroxylation process [6]. So chemical adsorption is further proved to exist.

4. Conclusion

Addition of α-Al$_2$O$_3$ can reduce the Si/Al ratio of geopolymer and takes influence on the microstructure and mechanical properties of the fly ash-based geopolymer products. α-Al$_2$O$_3$ addition with appropriate amount (such as 5 wt%) increases the geopolymerization extent. This results in higher compressive strength and surface area. A better level of structural ordering of amorphous geopolymer gel for sample with 5 wt% α-Al$_2$O$_3$ addition can also be observed through FTIR analysis. In contrast, excessive addition (such as 10 wt%) gives rise to the dramatic decrease of compressive strength and surface area.

The tests of formaldehyde adsorption capacity indicate that fly ash-based geopolymer products exhibit much better property of purifying indoor formaldehyde vapor than fly ash itself. Geopolymer gel takes the main role in adsorbing formaldehyde vapor through physical and chemical interactions between geopolymers and formaldehyde molecules.

Acknowledgements

References

[1] J. Davidovits, Geopolymer: inorganic polymeric new materials , J. Therm. Anal. 37 (1991) 633–1656.
[2] P. Duxson, A. Fernandez-Jimenez, J.L. Provis, G.C. Lukey, A. Palomo, J.S.J. van Deventer, Geopolymer technology: the current state of the art , J. Mater. Sci. 42 (2007) 917–2933.
[3] D. Khale, R. Chaudhary, Mechanism of geopolymerization and factors influencing its development: a review , J. Mater. Sci. 42 (2007) 29–746.
[4] H.K. Wu, P.J. Sun, New building materials from fly ash-based lightweight inorganic polymer , Constr. Build. Mater. 21 (2007) 211–217.
[5] M. Izquierdo, X. Querol, J. Davidovits, Coal fly ash-slag-based geopolymers: microstructure and metal leaching , J. Hazard. Mater. 166 (2009) 561–566.
[6] S.B. Wang, L. Lin, Z.H. Zhu, Solid-state conversion of fly ash to effective adsorbents for Cu removal from wastewater , J. Hazard. Mater. 139 (2007) 54–259.
[7] L. Lin, S.B. Wang, Z.H. Zhu, Geopolymeric adsorbents from fly ash for dye removal from aqueous solution , J. Colloid Interface Sci. 300 (2006) 52–59.
[8] K. Al-Zboon, M.S. Al-Harahsheh, F.B. Hani, Fly ash-based geopolymer for Pb removal from aqueous solution , J. Hazard. Mater. 188 (2011) 14–421.
[9] L. Zheng, W. Wang, Y.C. Shi, The effects of alkaline dosage and Si/Al ratio on the immobilization of heavy metals in municipal solid waste incineration fly ash-based geopolymer , Chemosphere 79 (2010) 665–671.
[10] P. Duxson, J.L. Provis, G.C. Lukey, S.W. Mallicoat, W.K. Kriven, J.S.J. van Deventer, Understanding the relationship between geopolymer composition, microstructure and mechanical properties , Colloids Surf. A 269 (2005) 47–58.
[11] K.L. Huang, Inorganic Chemistry , Science Press, Beijing, 2007.
[12] C.A. Rees, J.L. Provis, G.C. Lukey, The mechanism of geopolymer gel formation investigated through seeded nucleation , Colloids Surf. A 318 (2008) 97–105.
[13] U. Rattanasak, P. Chindaprasirt, Influence of NaOH solution on the synthesis of fly ash geopolymer , Miner. Eng. 22 (2009) 1073–1078.
[14] S. Songpiriyakij, T. Kubprasit, C. Jaturapitakkul, P. Chindaprasirt, Compressive strength and degree of reaction of biomass- and fly ash-based geopolymer , Constr. Build. Mater. 24 (2010) 236–240.
[15] B.M. Wittf, J.B. Uytterhoeven, Acid and alkaline sol–gel synthesis of amorphous aluminosilicates, dry gel properties, and their use in probing sol phase reactions , J. Colloids Interface Sci. 181 (1996) 200–207.
[16] E. Alvarez-Ayuso, X. Querol, F. Plana, A. Alastueya, N. Morenoa, M. Izquierdoa, O. Fonta, T. Morenoa, S. Dieza, E. Vázquezb, M. Barra, Environmental, physical and structural characterisation of geopolymer matrixes synthesised from coal (co-)combustion fly ashes , J. Hazard. Mater. 154 (2008) 175–183.
[17] A. Fernández-Jiménez, A. Palomo, Composition and microstructure of alkali activated fly ash binder: effect of the activator , Cem. Concr. Res. 35 (2005) 1984–1992.
[18] P. Duxson, G.C. Lukey, J.S.J. van Deventer, Evolution of gel structure during thermal processing of Na-geopolymer gels , Langmuir 22 (2006) 8750–8757.
[19] Y.S. Zhang, W. Sun, Z.J. Li, Composition design and microstructural characterization of calcined kaolin-based geopolymer cement , Appl. Clay Sci. 47 (2010) 271–275.
[20] F. Skvára, L. Kopeck, V. Smilauer, Zdenek Bittnar, Material and structural characterization of alkali activated low-calcium brown coal fly ash , J. Hazard. Mater. 168 (2009) 11–720.